

# Exploring Invariant Manifolds and Halo Orbits

Joseph D. Carpinelli \*

University of Maryland, College Park, Maryland, 20740

Low-cost trajectory design has been a subject of research for decades. Recently, researchers at California Polytechnic State University studied low-cost trajectory design through the use of invariant manifolds about Lagrange points in our solar system – a transfer from Earth to Jupiter, with an epoch similar to that of Voyager 1, was investigated [1]. This project aims to summarize, and at times replicate, the core concepts behind this manifold-based trajectory design. A general, analytical implementation for a Halo orbit solver is described, and implemented. A general, numerical implementation for a Halo orbit solver is described, and the preliminary code implementation is provided as a reference. This project was completed as part of the University of Maryland’s ENAE601 (Graduate Astrodynamics) course.

## Contents

I	Motivation	1
II	Introduction	1
II.A	Outline . . . . .	2
III	CR3BP Overview	2
III.A	Nondimensionalization . . . . .	2
III.B	Equations of Motion . . . . .	2
IV	Lagrange Points	2
IV.A	Manifolds about Lagrange Points . . .	3
IV.B	Orbits about Lagrange Points . . . . .	3
V	Halo Orbit Solutions	3
V.A	Analytical Halo Solution . . . . .	3
V.B	Numerical Halo Solution . . . . .	5
VI	Invariant Manifolds	5
VI.A	Overview . . . . .	5
VI.B	Algorithm . . . . .	5
VI.C	Usage . . . . .	6
VII	Conclusion	6
VIII	References	6
IX	Appendix	7

## I. Motivation

Halo orbits are stable and periodic within the Circular Restricted Three Body Problem, and can therefore provide satellites the benefit of reduced orbit maintenance fuel costs [7]. For these reasons, Halo orbits have been highly researched in recent years,

and will be utilized in upcoming NASA Artemis missions [9]. Separately, low cost trajectories are needed to design more efficient space exploration missions. One such method for low cost trajectory design utilizes invariant manifolds about Lagrange points in our solar system – this method has been shown, in one example, to decrease the required transfer  $\Delta v$  from Earth to Jupiter by approximately  $4 \frac{\text{km}}{\text{s}}$  when compared with the  $\Delta v$  of a transfer designed through patched conics [1].

Halo solutions are not easy to find – they are often quite difficult to solve for numerically. This topic’s complexity, coupled with it’s benefits to future low-cost interplanetary missions, motivates additional research.

## II. Introduction

Periodic, stable orbits are desirable for human spaceflight missions; eclipse avoidance, positioning for spacecraft communication and space science experiments, and data collection can be improved through robust orbit stability and periodicity or quasi-periodicity [8]. In the Circular Restricted Three-body Problem, several families of orbits are known which orbit Lagrange points. One such family of theoretically periodic orbits are known as Halo orbits; they are periodic within the Circular Restricted Three-body Problem, and quasi-periodic in higher fidelity ephemeris models [8] [1]. This periodicity makes Halo orbits attractive candidates for target orbits in future space missions. Unfortunately, finding Halo orbits is not trivial. An analytical solution, as described by Rund, can provide an initial estimate for a particular Halo orbit [1]. However, numerically

---

\*Graduate Assistant, Department of Aerospace Engineering, University of Maryland

propagating this analytical solution will result in a non-periodic orbit. A numerical algorithm has been developed to iterate from this aperiodic initial orbit to a nearby, periodic orbit [1] [2].

Halo orbits' connection with Lagrange points results in an additional, exploitable characteristic: invariant manifolds. Collections of trajectories approach, and depart periodic orbits about Lagrange points. Groups of trajectories which approach the Halo orbit are known as stable invariant manifolds, while groups of trajectories which depart the Halo orbit are known as unstable invariant manifolds [1]. These trajectories can be utilized by a spacecraft for low-cost travel along the manifold.

This project implements the analytical Halo solution in Julia, a scientific computing language. Several analytical Halo orbits are presented, and rough estimates for their numerical solutions are also shown. Note that neither of these estimates are truly periodic when used as inputs to a Circular Restricted Three-body propagator. The summarized numerical Halo orbit solver must be applied to these initial conditions to find close-by, truly periodic orbits [1] [2].

#### A. Outline

First, the Circular Restricted Three-body Problem (CR3BP) and Lagrange points will be reviewed, and the added context of invariant manifolds will be presented. Next, Halo orbits will be introduced, and analytical and numerical methods for solving Halo orbits will be summarized [1] [2]. Finally, invariant manifolds about Halo orbits will be summarized, and low-cost manifold-based interplanetary transfer designs will be summarized, as presented by Rund et al [1].

### III. CR3BP Overview

The Circular Restricted Three-body Problem is an orbital mechanics simplification. Within this domain, a spacecraft of infinitesimal mass is accelerated by two celestial bodies.

#### A. Nondimensionalization

Initial conditions are often provided, and propagated, in non-dimensional form. This nondimensionalization is completed by dividing all position units by the distance between the two celestial bodies, and dividing all time units by a user-specified duration [3]. These nondimensionalizations are shown in equations (1) and (2) below, where subscript  $N,s$  denotes the nondimensional state of the spacecraft with respect to the center of mass of the two celestial bodies (COM),

and subscript  $D,s$  denotes the dimensional state of the spacecraft with respect to COM. The single nondimensional mass parameter is labeled  $\mu$ , while  $\mu_1$  and  $\mu_2$  are the dimensioned mass parameters for the first and second celestial bodies respectively.

$$\vec{r}_{N,s} = \vec{r}_{D,s} \times \frac{1}{DU} \quad (1)$$

$$\vec{v}_{N,s} = \vec{v}_{D,s} \times \frac{DT}{DU} \quad (2)$$

$$\mu = \frac{\min(\mu_1, \mu_2)}{\mu_1 + \mu_2} \quad (3)$$

#### B. Equations of Motion

The nondimensional equations of motion for a spacecraft within the Circular Restricted Three-body Problem are shown in equations (4), (5), and (6) below [3].

$$\ddot{x} = 2\dot{y} + x - \frac{(1-\mu)(x+\mu)}{r_1^3} - \frac{\mu(x-1+\mu)}{r_2^3} \quad (4)$$

$$\ddot{y} = -2\dot{x} + y - \frac{(1-\mu)y}{r_1^3} - \frac{\mu y}{r_2^3} \quad (5)$$

$$\ddot{z} = -\frac{(1-\mu)z}{r_1^3} - \frac{\mu z}{r_2^3} \quad (6)$$

$$r_1 = \sqrt{(x+\mu)^2 + y^2 + z^2}$$

$$r_2 = \sqrt{(x+\mu-1)^2 + y^2 + z^2}$$

### IV. Lagrange Points

Lagrange points are equilibrium points within the Circular Restricted Three-body Problem. There are 5 equilibrium positions for each CR3BP system [3]. Their general equations are shown below [1]. All L1, L2, and L3 Lagrange points are of the form  $(x^*, 0, 0)$ , and the L4 and L5 Lagrange points are of the form  $(x^*, y^*, 0)$ . The Lagrange points for the Earth-Moon CR3BP system are shown in Figure 1, which replicates Figure 2.2 in Rund et al's [1].

$$L_1 : x - \frac{(1-\mu)}{(x+\mu)^2} + \frac{\mu}{(x+\mu-1)^2} = 0 \quad (7)$$

$$L_2 : x - \frac{(1-\mu)}{(x+\mu)^2} - \frac{\mu}{(x+\mu-1)^2} = 0 \quad (8)$$

$$L_3 : x + \frac{(1-\mu)}{(x+\mu)^2} + \frac{\mu}{(x+\mu+1)^2} = 0 \quad (9)$$

$$L_4 : x = \frac{1}{2} - \mu, y = \frac{\sqrt{3}}{2} \quad (10)$$

$$L_5 : x = \frac{1}{2} - \mu, y = \frac{-\sqrt{3}}{2} \quad (11)$$

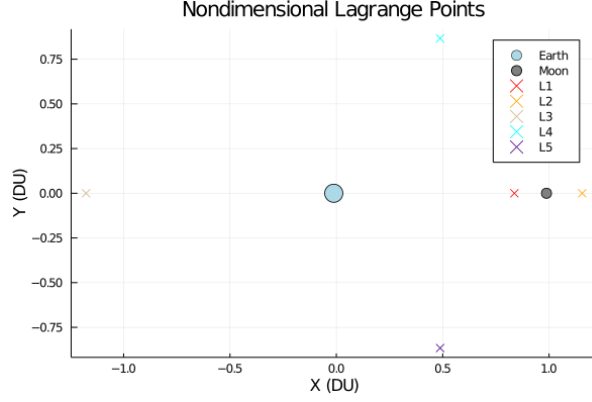


Fig. 1 Earth-Moon Lagrange Points

In general, equilibrium positions for nonlinear systems can be stable or unstable. Lagrange points are no exception – perturbing a spacecraft at a stable Lagrange point will result in the spacecraft returning to that equilibrium position, while perturbing a spacecraft at an unstable Lagrange point will result in the spacecraft continuing to diverge from the equilibrium position. Collections of trajectories that diverge from, or converge to Lagrange points are known as manifolds [1]. Figure 2 shows one such example of a divergent conditions at an Earth-Moon Lagrange point [1].

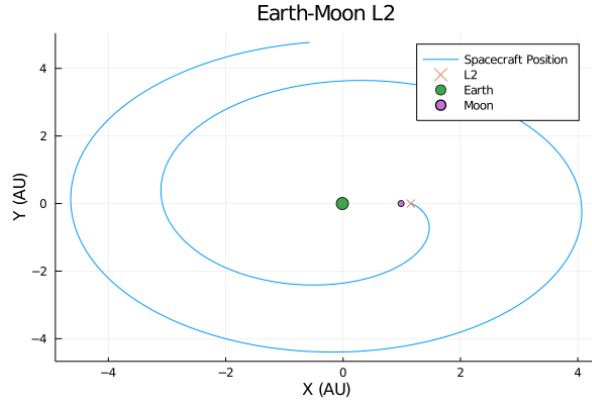


Fig. 2 Divergent Trajectory near Sun-Earth L2

#### A. Manifolds about Lagrange Points

As previously mentioned, there exist collections of trajectories near Lagrange points which approach, and depart each Lagrange point. These collections of trajectories are known as manifolds [1]. To compute one such trajectory, the eigenvectors of the Jacobian of the state vector at the Lagrange point can be used to find perturbations which would place the spacecraft within a manifold [1]. This use of eigenvectors is a fa-

miliar concept in linear analysis. For a linear system, the eigenvectors of the zero-input dynamics specify how each state excites each dynamical mode.

The Jacobian of the state vector at a Lagrange point will produce two oscillatory pairs of eigenvalues, and one pair of real eigenvalues [1]. The span of the eigenvector corresponding to the larger real eigenvalue represents the perturbations which would move a spacecraft from a Lagrange point to an unstable manifold. The span of the eigenvector corresponding to the smaller real eigenvalue represents the perturbations which would move a spacecraft from the Lagrange point to a stable manifold [1]. Expressions for the Jacobian of the state vector, and perturbing initial conditions for the stable and unstable manifolds near a Lagrange point are shown below [1].

$$J = \begin{bmatrix} 0 & 0 & 0 & 1 & 0 & 0 \\ 0 & 0 & 0 & 0 & 1 & 0 \\ 0 & 0 & 0 & 0 & 0 & 1 \\ \frac{\partial \ddot{x}}{\partial x} & \frac{\partial \ddot{x}}{\partial y} & \frac{\partial \ddot{x}}{\partial z} & 0 & 2 & 0 \\ \frac{\partial \ddot{y}}{\partial x} & \frac{\partial \ddot{y}}{\partial y} & \frac{\partial \ddot{y}}{\partial z} & -2 & 0 & 0 \\ \frac{\partial \ddot{z}}{\partial x} & \frac{\partial \ddot{z}}{\partial y} & \frac{\partial \ddot{z}}{\partial z} & 0 & 0 & 0 \end{bmatrix} \quad (12)$$

$$X_{\text{STABLE}} = X \pm \epsilon V_{\text{STABLE}} \quad (13)$$

$$X_{\text{UNSTABLE}} = X \pm \epsilon V_{\text{UNSTABLE}} \quad (14)$$

#### B. Orbits about Lagrange Points

Several families of orbits are known which orbit Lagrange points – these orbits are known as Libration orbits [1]. Common Libration orbits include Lyapunov orbits, Halo orbits, and Lissajous orbits; each are briefly summarized by Rund, and their descriptions are paraphrased here [1]. Lyapunov orbits are two-dimensional, Halo orbits are periodic and three-dimensional, and Lissajous orbits are “quasi-periodic” and three-dimensional [1].

### V. Halo Orbit Solutions

Solving for a Halo orbit is difficult, as the computations are incredibly numerically sensitive. An iterative, numerical algorithm has been developed to find a three-dimensional, periodic orbit near a provided initial guess [1] [2]. As Rund shows, an analytical solution can be used as the initial guess [1].

#### A. Analytical Halo Solution

Rund outlines an analytical solution for a Halo orbit, given a Z-amplitude and non-dimensional mass parameter  $\mu$ , in great detail in section 3.2 [1]. The algorithm first sets parameter values corresponding

to the selected Lagrange point; only L1 and L2 analytical Halo orbits can be found with this algorithm. Then, the algorithm plugs these parameters into a general equation of motion. The distance from the CR3BP center of mass to the selected Lagrange point must be added to all  $x$  values, as the algorithm calculates all positions with respect to the selected Lagrange point [1]. Rund's explanation is excellent and complete, so it will not be explained in more detail here.

I implemented this analytical Halo solution with

Julia code, as shown in Appendix A. The analytical solutions can also show the approximate shape of a Halo orbit. The analytical algorithm requires an input for  $Z$  amplitude of the Halo orbit; Rund uses a dimensional  $Z$  amplitude as an input, and my implementation takes a non-dimensional  $Z$  amplitude [1]. Four examples of analytical solutions for families of Halo orbits are shown in Figure 3, Figure 4, Figure 5, and Figure 6. They were computed using my implementation of the analytical algorithm [1].

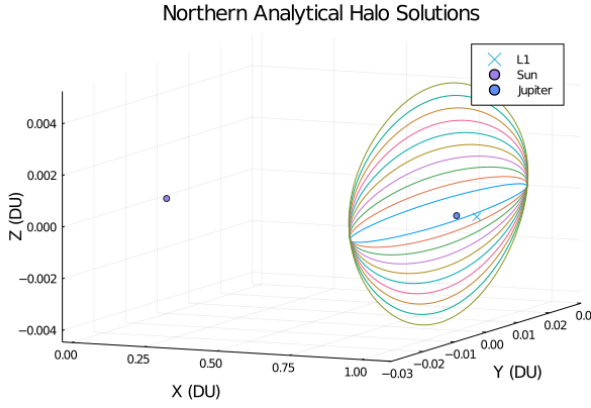


Fig. 3 Northern Halo Orbits about Sun-Jupiter L1

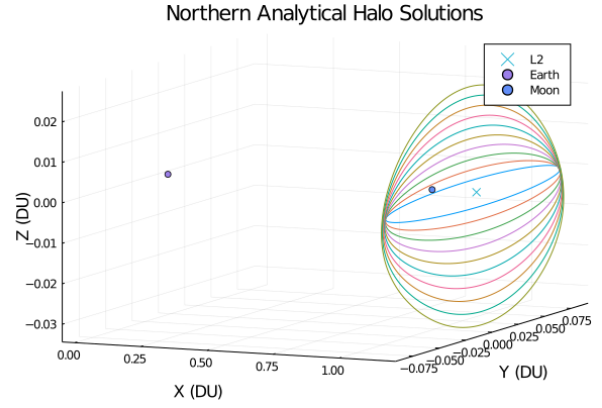


Fig. 5 Northern Halo Orbits about Earth-Moon L2

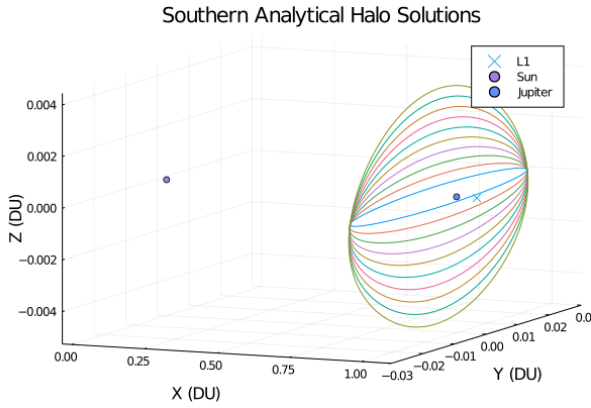


Fig. 4 Southern Halo Orbits about Sun-Jupiter L1

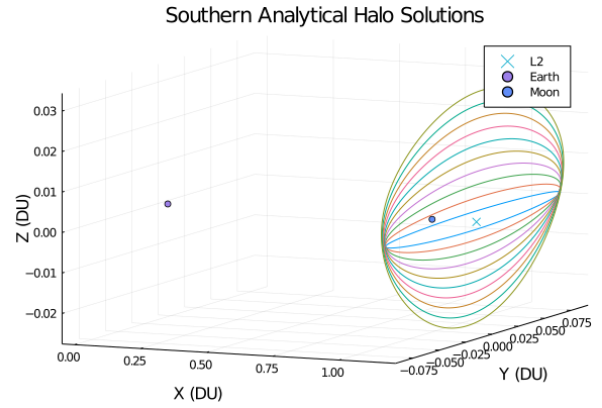


Fig. 6 Southern Halo Orbits about Earth-Moon L2

## B. Numerical Halo Solution

With the  $t = 0$  step of the analytical Halo solution in-hand, we can use the numerical Halo solution to iteratively find a close estimate to a periodic Halo orbit [1]. This algorithm is presented in literature, including by Howell and Rund [2] [1]. This algorithm is also presented in Lecture 16 of the University of Maryland's Graduate Astrodynamics course, ENAE601. For this reason, this section does not go into the algorithm in complete detail. Instead, it provides a broad overview. Rund provides a more complete and detailed explanation [1].

The numerical algorithm involves iterative propagation. Source code in Julia is available in Appendix B. The analytical algorithm should have produced a state vector of the following form:

$$\vec{x} = \begin{bmatrix} x_0^* & 0 & z_0^* & 0 & \dot{y}_0^* & 0 \end{bmatrix}^T$$

We will need to iterate on this initial guess to find a numerically periodic Halo orbit. The form of our subsequent guesses will stay the same, but our  $x_0$  and  $\dot{y}_0$  values will change. We could instead choose to change our  $z_0$  and  $\dot{y}_0$  values, but in this description the former option will be used [1] [2].

To find a new initial state guess, we can use linear analysis techniques to find state delta values which will move the solutions in the desired direction. We can use the state transition matrix  $\Phi$  for this purpose. In the context of the Circular Restricted Three-body Problem, the state transition matrix  $\Phi$  relates the initial state vector to the state vector at each future time  $t$  [1]. The state transition matrix dynamics are described by  $\dot{\Phi} = F\Phi$ , where  $F$  is a  $6 \times 6$  block matrix with zeros at the top left, the identity matrix at the top right, the Hessian (matrix of second partial derivatives) of the potential energy of the spacecraft at the bottom left, and a constant matrix at the bottom right [1].

$$F = \begin{bmatrix} 0 & I_3 \\ U_{XX} & 2\Omega \end{bmatrix} \quad (15)$$

$$\Omega = \begin{bmatrix} 0 & 1 & 0 \\ -1 & 0 & 0 \\ 0 & 0 & 0 \end{bmatrix} \quad (16)$$

$$U_{XX} = \begin{bmatrix} \frac{\partial^2 U}{\partial x \partial x} & \frac{\partial^2 U}{\partial x \partial y} & \frac{\partial^2 U}{\partial x \partial z} \\ \frac{\partial^2 U}{\partial y \partial x} & \frac{\partial^2 U}{\partial y \partial y} & \frac{\partial^2 U}{\partial y \partial z} \\ \frac{\partial^2 U}{\partial z \partial x} & \frac{\partial^2 U}{\partial z \partial y} & \frac{\partial^2 U}{\partial z \partial z} \end{bmatrix} \quad (17)$$

With the equations above defined, we have all we need to complete the numerical algorithm. The initial state transition matrix is set to the identity matrix,

and each row is appended to the state vector. As a result, the total state vector for this numerical integration contains 42 variables. We numerically integrate the initial state vector until the solution crosses the  $x - z$  axis (that is, when  $y = 0$ ). We then add the following state deltas to our initial condition, and repeat the procedure until the values  $\dot{x}$  and  $\dot{z}$  are within some tolerance near zero [1]. After this procedure finishes, we should be left with an initial condition vector for a periodic Halo orbit. This orbit may still diverge after several periods of numerical integration, depending on how small our numerical tolerance was set [1].

$$\delta \dot{x} = -\dot{x}, \quad \delta \dot{z} = -\dot{z} \quad (18)$$

$$\begin{bmatrix} \delta x_0 \\ \delta \dot{y}_0 \end{bmatrix} = \left( \begin{bmatrix} \Phi_{41} & \Phi_{45} \\ \Phi_{61} & \Phi_{65} \end{bmatrix} - \frac{1}{\dot{y}} \begin{bmatrix} \ddot{x} \\ \ddot{z} \end{bmatrix} \right)^{-1} \begin{bmatrix} \delta \dot{x} \\ \delta \dot{z} \end{bmatrix} \quad (19)$$

## VI. Invariant Manifolds

### A. Overview

Each point along the periodic Halo orbit is connected with an unstable and stable invariant manifold – this manifold is a collection of spacecraft trajectories which converge to the point on the Halo orbit (stable manifold), or diverge from the point on the Halo orbit (unstable manifold) [1]. We could calculate the eigenvectors of the Jacobian at each time step to give us the range of perturbations which would shift the spacecraft onto the manifold, as previously discussed. As Rund points out, this is very computationally expensive. Instead, we can use the monodromy matrix – the state transition matrix after one period  $T$  [1].

### B. Algorithm

To find the range of perturbations (in state space) which will shift the spacecraft onto the unstable or stable manifolds at each time step along the Halo orbit, we simply need to numerically integrate the full 42 element state vector (with  $\Phi$  set to the identity matrix as an initial value) for one full period. We then note the monodromy matrix is equivalent to the final state transition matrix. The eigenvector associated with the maximum eigenvalue of the monodromy matrix,  $V^U$ , is used to find perturbations to reach the unstable manifold, and the eigenvector associated with the minimum eigenvalue,  $V^S$ , is used to find perturbations to reach the stable manifold at each time step  $i$ , and some small scalar perturbation magnitude  $\epsilon$  [1]. This is shown in equations (20) through (24).

### C. Usage

Once the perturbing state delta has been found for each time step, and for both the unstable and stable invariant manifolds, we can numerically integrate many trajectories along each point in the Halo orbit to visualize the stable and unstable invariant manifolds. This can be seen in Rund’s Figure 3.6 [1]. Trajectories within unstable manifolds are propagated forward in time, and trajectories within stable manifolds are propagated backwards in time. As Rund shows, these invariant manifolds about Halo orbits can be utilized to form low-cost transfers from one Halo orbit to another [1]. Substantial  $\Delta v$  savings are reported when compared with traditional trajectory design methods; Rund’s Masters Thesis provides more detail [1].

$$V_i^S = \Phi(t_0 + t_i, t_0)V^S \quad (20)$$

$$V_i^U = \Phi(t_0 + t_i, t_0)V^U \quad (21)$$

$$X_i^S = X_i \pm \epsilon \frac{V_i^S}{|V_i^S|} \quad (22)$$

$$X_i^U = X_i \pm \epsilon \frac{V_i^U}{|V_i^U|} \quad (23)$$

$$M = \Phi(t_0 + T, t_0) \quad (24)$$

## VII. Conclusion

Halo orbits have many desirable properties [8] [1]. They are also incredibly difficult to find numerically with high precision. A method for finding analytical solutions for Halo orbits was summarized and implemented [1]. A method for iterating on this analytical initial guess to find a numerically periodic Halo orbit was summarized and implemented, though the implemented code is not fully functional [1] [2].

Common linear analysis techniques can be used to find manifolds about Halo orbits [1] [2]. These manifolds can then be utilized to form low-cost transfers between Halo orbits [1]. Future work includes fixing the numerical Halo solver code, and exploring potential cost benefits for different interplanetary transfers.

## VIII. References

- [1] Rund, M. S., “Interplanetary Transfer Trajectories Using the Invariant Manifolds of Halo Orbits,” , 2018.
- [2] Howell, K. C., “Three-dimensional, periodic, ‘halo’ orbits,” *Celestial mechanics*, Vol. 32, No. 1, 1984, pp. 53–71.
- [3] Vallado, D. A., *Fundamentals of astrodynamics and applications*, Vol. 12, Springer Science & Business Media, 2001.
- [4] Lara, M., Russell, R., and Villac, B., “Classification of the distant stability regions at Europa,” *Journal of Guidance, Control, and Dynamics*, Vol. 30, No. 2, 2007, pp. 409–418.
- [5] Richardson, D., “Analytical construction of periodic orbits about the collinear points of the Sun-Earth system.” *asdy*, 1980, p. 127.
- [6] Koon, W. S., Lo, M. W., Marsden, J. E., and Ross, S. D., “Dynamical systems, the three-body problem and space mission design,” Free online Copy: Marsden Books, 2008.
- [7] Williams, J., Lee, D. E., Whitley, R. J., Bokelmann, K. A., Davis, D. C., and Berry, C. F., “Targeting cislunar near rectilinear halo orbits for human space exploration,” 2017.
- [8] Zimovan-Spreen, E. M., Howell, K. C., and Davis, D. C., “Near rectilinear halo orbits and nearby higher-period dynamical structures: orbital stability and resonance properties,” *Celestial Mechanics and Dynamical Astronomy*, Vol. 132, No. 5, 2020, pp. 1–25.
- [9] NASA, *NASA’s Lunar Exploration Program Overview*, 2020.
- [10] Carpinelli, J., “UnitfulAstrodynamics.jl,” <https://juliahub.com/ui/Packages/UnitfulAstrodynamics/uJGLZ/>, 2020.

## IX. Appendix

Code to evaluate analytical and numerical Halo solutions are shown below. Only the analytical function is working at the time of writing. If the unicode characters in variables names are cutoff in your PDF version of this document, you can find the same code on GitHub at [cadojo/UnitfulAstrodynamics.jl](https://github.com/cadojo/UnitfulAstrodynamics.jl). The numerical function, "halo", currently has bugs that have not yet been resolved. All orbits produced by this function seem to be shifted such that they are no longer encircling the Lagrange point.